General Methods for Geometry and Wave Function Optimization

Thomas H. Fischer

Interdisziplinäres Projektzentrum für Supercomputing, ETH-Zentrum, 8092 Zürich, Switzerland

and Jan Almlöf*

Minnesota Supercomputer Institute, University of Minnesota, Minneapolis, Minnesota 55455
(Received: April 20, 1992)

A combination of variable-metric second-order update schemes and the DIIS method for both geometry and Hartree–Fock wave function optimization is described. A recursive procedure for updating large Hessians is presented. The performances of geometry optimizations with respect to the choice of the coordinate system (symmetry-adapted, internal, and Cartesian coordinates), the initial nuclear Hessian, and the optimization procedure have been investigated by a series of benchmark molecules. Formulas for the generation of initial nuclear Hessians are given.

I. Introduction

The development of high-performance computer technology, along with substantial progress in methods and algorithms, has substantially extended the applicability of LCAO-MO ab initio methods. For the treatment of large molecular systems, direct methods[1,2] are especially efficient. These methods have already made very large calculations possible, both at the Hartree–Fock and the MP2 level.

For any iterative SCF calculation it is essential to minimize the number of iterations required to reach self-consistency. This is particularly important in direct approaches where the recalculation of integrals in every iteration is necessary. Variable-metric, second-order (SO) methods for minimizing the energy expression using an exponential parameterization of the orbital rotations are powerful tools to converge Hartree–Fock (HF) wave functions at a given geometry.[3-5] However, these methods normally require the storage of an approximate inverse second derivative matrix with respect to the orbital rotations (orbital Hessian) which can become very large for extended systems. In this paper we will outline a recursive procedure that allows the update of the information contained in the orbital Hessian without storing the full matrix.

Another widely used procedure for convergence acceleration in wave function optimization is the DIIS (direct inversion in the iterative subspace) interpolation algorithm.[6] In this work we will also describe an alternative DIIS formulation that is based on the orbital rotation idea. This algorithm can be combined with the variable-metric second-order methods mentioned before. It is possible to reuse the orbital Hessian accumulated by various update procedures in calculations on nearby geometries, and we will investigate this method regarding geometry optimization.

Geometry optimizations, i.e., the determination of stationary points of a potential energy hypersurface, can be performed for large molecules by means of the analytical calculation of the energy gradient with respect to the nuclear coordinates. Fast convergence of the geometry parameters is essential because the evaluation of the nuclear gradient is computationally expensive. In addition to the SCF convergence acceleration we will discuss also the combination of second-order update methods and the geometry DIIS interpolation procedure[7,8] for geometry optimizations.

A problem closely related to geometry optimizations is that of locating transition states on a potential energy surface. While the examples given in the present paper deal exclusively with minima, it is worth noting that the DIIS method is not restricted to such cases. Specifically, the problem of locating transition states using a DIIS method has been addressed in a recent paper.[9]

The rate of convergence of a geometry optimization depends not only on the optimization procedure but also on the initial guess of nuclear Hessian. This is particularly important for molecules with shallow potentials, such as weakly interacting complexes. Computationally inexpensive empirical methods to generate initial nuclear Hessians have been proposed by Schlegel.[10] We present alternative formulas to estimate an initial nuclear Hessian more suited for hydrogen-bonded complexes. The comparison of different coordinate systems for geometry optimizations, i.e., symmetry-adapted internal coordinates or Cartesian coordinates, will also be discussed by means of a series of benchmark molecules. The methods described in this paper have been implemented in the program package DISCO.[11]

II. Optimization Procedure

A. SCF Convergence Acceleration. The possibility to combine the variable-metric method and the DIIS algorithm was mentioned in the early work by Csaszar and Pulay[7] but has not attracted much attention since then. In this first section we will describe the combination of the variable-metric second-order convergence scheme and the DIIS interpolation procedure for Hartree–Fock wavefunctions. Second-order update methods attempt to augment the approximate inverse Hessian $\mathbf{H}_{n-1}$ with second derivative information gained in the $(n-1)$th iteration so that $\mathbf{H}_n$ is a better guess for the exact inverse Hessian. $\mathbf{H}_n$ is chosen in such a way that the quasi-Newton condition is achieved

$$\mathbf{H}_n \cdot \Delta_{n-1} = \delta_{n-1} \tag{1}$$

where

$$\Delta_{n-1} = \nabla_n - \nabla_{n-1}$$

∇ is the gradient vector and δ the displacement vector.

The most successful applied update procedure is the Broyden–Fletcher–Goldfarb–Shanno (BFGS) algorithm[12]

$$\mathbf{H}_n = \mathbf{H}_{n-1} + \mathbf{E}_{n-1} \tag{2a}$$

$$E_{n-1} = (1 + \alpha \Delta^{\mathrm{T}}_{n-1} \cdot \mathbf{v}) \alpha \delta_{n-1} \delta^{\mathrm{T}}_{n-1} - \alpha(\delta_{n-1} \mathbf{v}^{\mathrm{T}} + \mathbf{v} \delta^{\mathrm{T}}_{n-1}) \tag{2b}$$

where

$$\mathbf{v} = \mathbf{H}_{n-1} \Delta_{n-1}$$

$$\alpha = (\delta^{\mathrm{T}}_{n-1} \cdot \Delta_{n-1})^{-1}$$

The new displacement vector is obtained by

$$\delta_n = -\mathbf{H}_n \cdot \nabla_n \tag{3}$$

The parameters optimized in the SCF procedure are the orbital coefficients. These coefficients are in general not independent, since orthonormality criteria have to be fulfilled. However, the orbital rotations between occupied and virtual orbitals can be expressed with an independent set of parameters, e.g., through an exponential parameterization procedure.[3,4] These are the parameters to be optimized. Their number is equal to the product of the number of occupied and virtual orbitals or reduced by a certain factor if symmetry is present. Thus, the orbital Hessian required for a second-order algorithm becomes quite large for

0022-3654/92/2096-9768$03.00/0

extended systems with low symmetry. In a second-order update procedure the inverse Hessian has to be both updated (eq 2) from one iteration to the next and multiplied by the gradient vector (eq 3) to obtain the new displacements. In the first step an initial diagonal orbital Hessian $\mathbf{H}_{start}$ can be estimated by transforming the Fock matrix into an MO basis and diagonalizing it.[5] Since the memory required for storing the full, nonsparse Hessian (or its inverse) is often prohibitive, it has been suggested[5] to store the inverse Hessian in the small, expanding subspace spanned by the gradients at each point. In the following we describe a procedure where the inverse orbital Hessian can be updated and multiplied by a general vector v without storing the full matrix. The algorithm is based on the fact that the product of the inverse Hessian of the nth iteration and a vector can be evaluated recursively by using inverse Hessians, gradients, and displacements from all previous iterations

$$\mathbf{H}_n \cdot \mathbf{v} = \mathbf{H}_{start} \cdot \mathbf{v} + \sum_{i=1}^{n-1} \mathbf{E}_i \cdot \mathbf{v} \tag{4}$$

where $\mathbf{H}_{start}$ can be a diagonal or sparse matrix and has to be stored. $\mathbf{E}_i$ can be obtained by the BFGS formula or any similar update method.

The recursion algorithm using the BFGS formalism can be viewed as follows:

(1) Initialize the demanded vector $\mathbf{w} = \mathbf{H}_{start}\mathbf{v}$

(2) If $n = 1$ return

(3) Evaluate

$$\Delta_{n-1} = \nabla_n - \nabla_{n-1}$$

and initialize

$$\mathbf{y}_{n-1} = \mathbf{H}_{start} \cdot \Delta_{n-1}$$

(4) Loop $i = 1$ to $n - 2$

evaluate the dot products

$$S_1 = \frac{1}{\delta_i^T \cdot \Delta_i}; \qquad S_2 = \frac{1}{\Delta_i^T \cdot \mathbf{y}_i}; \qquad S_3 = \delta_i^T \cdot \mathbf{v}$$

$$S_4 = \mathbf{y}_i^T \cdot \mathbf{v}; \qquad S_5 = \delta_i^T \cdot \Delta_{n-1}; \qquad S_6 = \mathbf{y}_i^T \cdot \Delta_{n-1}$$

$$T_1 = \left(1 + \frac{S_1}{S_2}\right) S_1 S_3 - S_1 S_4; \quad T_2 = S_1 S_3$$

$$T_3 = \left(1 + \frac{S_1}{S_2}\right) S_1 S_5 - S_1 S_6; \quad T_4 = S_1 S_5$$

calculate $\mathbf{y}_{n-1}$ and w recursively

$$\mathbf{w} = \mathbf{w} + T_1 \delta_i - T_2 \mathbf{y}_i$$

$$\mathbf{y}_{n-1} = \mathbf{y}_{n-1} + T_3 \delta_i - T_4 \mathbf{y}_i$$

End loop i

(5) Evaluate the dot products

$$S_1 = \frac{1}{\delta^T_{n-1} \cdot \Delta_{n-1}}; \qquad S_1 = \frac{1}{\Delta^T_{n-1} \cdot \mathbf{y}_{n-1}};$$

$$S_3 = \delta^T_{n-1} \cdot \mathbf{v}; \quad S_4 = \mathbf{y}^T_{n-1} \cdot \mathbf{v}$$

$$T_1 = \left(1 + \frac{S_1}{S_2}\right) \mathbf{S}_1 \mathbf{S}_3 - \mathbf{S}_1 \mathbf{S}_4; \; T_2 = S_1 S_3$$

update the vector w

$$\mathbf{w} = \mathbf{w} + T_1 \delta_{n-1} - T_2 \mathbf{y}_{n-1}$$

(6) Return.

In this procedure, the three vectors δ, y, and Δ have to be stored in every SCF iteration, along with the (sparse) initial inverse Hessian. The storage of the full inverse Hessian would require $m_o(m_o + 1)/2$ words of memory or disk space, where m_o is the number of possible orbital rotations, and would be prohibitive for many molecules and computer configurations. With this recursive method only $m_o(3n_{tot} + 1)$ elements have to be stored, where n_{tot} is the total number of SCF iterations, typically not more than 20 per energy evaluation. The computer time required for the recursive update is only a couple of seconds on an IBM 3090 computer for a medium size molecule with about 10^4 orbital rotations.

The DIIS interpolation method normally used for wave function optimization is based on a linear combination of density matrices from previous iterations.[6] A special adaptation of the DIIS procedure for geometry optimization has been reported, the so-called GDIIS.[7] This idea can be used for the wavefunction optimization as well. It uses linear combinations of orbital rotation parameter vectors $\mathbf{x}_1, \mathbf{x}_2, \ldots, \mathbf{x}_m$ generated in previous iterations to find the best parameter vector in this m-dimensional subspace. This leads to a system of $m + 1$ linear equations

$$\begin{bmatrix} A_{11} & \cdots & A_{1m} & 1 \\ \cdots & & & \cdots \\ A_{m1} & \cdots & A_{mn} & 1 \\ 1 & \cdots & 1 & 0 \end{bmatrix} \begin{bmatrix} c_1 \\ \cdots \\ c_m \\ \lambda \end{bmatrix} = \begin{bmatrix} 0 \\ \cdots \\ 0 \\ 1 \end{bmatrix} \tag{5}$$

where $A_{ij} = \langle \mathbf{e}_i, \mathbf{e}_j \rangle$, $i, j = 1, \ldots, m$

$$\mathbf{e}_i = -\mathbf{H}_n \cdot \nabla_i$$

and λ is a Lagrangian multiplier.

The new displacements are obtained by

$$\delta_n = \mathbf{x}_n^* - x_{n-1} - \mathbf{H}_n \cdot \nabla_n^* \tag{6}$$

where

$$x_n^* = \sum_{i=1}^{m} c_i \mathbf{x}_i; \qquad \nabla_n^* = \sum_{i=1}^{m} c_i \nabla_i$$

In our DIIS implementation we gradually discard information older than m iterations (default: $m = 4$) to improve the adjustment to the actual surface. We have found this default to provide a reasonable compromise for a large number of cases. Obviously, a too large value of m will be counterproductive on surfaces with rapidly varying Hessians (large anharmonicity). For more harmonic potentials a larger value will be more efficient, but in these cases convergence is usually obtained in few iterations anyway, and the exact value of m is then irrelevant in practice. The combined second-order update/DIIS (SO/DIIS) method updates the approximate inverse Hessian in a first step. Then the new displacements are obtained by the DIIS procedure using the updated Hessian. For the generation of the matrix A (see eq 5) and for the displacement vectors (eq 6) within the DIIS procedure the updated inverse Hessian has to be multiplied by various vectors. This can be achieved by the recursive scheme outlined above and there is no need to have the Hessian explicitly.

B. Convergence Acceleration for the Geometry Optimization. With small modifications the SO/DIIS procedure for HF wave functions can be applied to geometry optimization, if geometry parameters, nuclear gradient, and nuclear Hessian are used instead of orbital rotations, orbital gradient, and orbital Hessian. Because the number of independent geometry parameters is much less than the number of orbital rotations, the nuclear Hessian can be stored and there is no need for a recursive Hessian update procedure.

For both the wave function and geometry optimization within the SO/DIIS method, an initial estimated Hessian is required. An empirical nuclear Hessian matrix for a chosen set of internal coordinates can be estimated from a redundant set of individual internal force constants as suggested by Schlegel[10]

$$\mathbf{h}^{cart}_{start} = \mathbf{B}^T_{red} \mathbf{h}_{red} \mathbf{B}_{red} \tag{7}$$

$$\mathbf{h}_{start} = (\mathbf{B}^T)^{-1} \mathbf{h}^{cart}_{start} \mathbf{B}^{-1}$$

where $\mathbf{B}$ is the transformation matrix between Cartesian and internal coordinates[13,14] and $\mathbf{h}_{red}$ is a diagonal matrix containing the individual force constants (see Table I). The redundant individual internal coordinates are usually chosen in such a way that they include all stretch, bend, torsion, and out-of-plane co-

TABLE I: Empirical Formulas for Individual Force Constants (in hartree/bohr² or hartree/rad²) Used To Estimate the Nuclear Hessian for Geometry Optimizations

Bond stretch between atoms a and b:

$$h_{stre} = A \exp\{-B(r_{ab} - r_{cov}^{ab})\}$$

r, bond length

r_{cov}, sum of covalent radii

$A = 0.3601$; $B = 1.944$

Valence angle bend formed by atoms b–a–c:

$$h_{bend} = A + \frac{B}{[r_{cov}^{ab} r_{cov}^{ac}]^D} \exp\{-C(r_{ab} + r_{ac} - r_{cov}^{ab} - r_{cov}^{ac})\}$$

$A = 0.089$; $B = 0.11$; $C = 0.44$; $D = -0.42$

Torsion about the central bond between atoms a and b:

$$h_{tors} = A + \frac{BL^D}{[r_{ab} r_{cov}^{ab}]^E} \exp\{-C(r_{ab} - r_{cov}^{ab})\}$$

L, number of bonds connected to atom a and b (except the central bond)

$A = 0.0015$; $B = 14.0$; $C = 2.85$; $D = 0.57$; $E = 4.00$

Out-of-plane bend of atom x and the plane formed by atoms a, b, and c where atom x is connected to atom a

$$h_{outp} = A + B[r_{cov}^{ab} r_{cov}^{ac}]^E (\cos \Phi)^D \exp\{-C(r_{ax} - r_{cov}^{ax})\}$$

Φ, out-of-plane angle

$A = 0.0025$; $B = 0.0061$; $C = 3.00$; $D = 4.00$; $E = 0.80$

ordinates which can be formed by the bonded atoms. Extending the method proposed by Schlegel,[10] we have found it more efficient to use different formulas for the individual force constants (see Table I). A diagonal hydrogen-bond stretch force constant may differ by more than an order of magnitude from a regular chemical bond stretch constant. This is also the case for valence angle bend, torsion, and out-of-plane diagonal force constants. The formulas recommended by Schlegel for a torsion of a hydrogen bond may lead to a negative diagonal force constant. The purpose of our proposed modification is to obtain more reasonable force constants, especially for weak interacting complexes. As discussed elsewhere, the generation of cubic force constants is also possible, using almost the same formulas with a different parameterization. The present parameters have been obtained from calculations on a series of reference molecules optimized mainly on 6-31G** basis set level.

Very important for the progress of the geometry optimization is the choice of the coordinate system in which the optimization is performed.[10] Since the estimation of off-diagonal force constants is generally uncertain in any coordinate system, it is desirable to use one where the approximate nuclear Hessian is almost diagonal or blocked such that different subsets of the coordinates can be optimized independently of each other. If point-group symmetry is present, symmetry-adapted internal coordinates provide an obvious such choice. Symmetry constraints on the geometry can easily be applied by only considering variations in the totally symmetric coordinates. In molecules with simple topology, the Eckart criteria are automatically fulfilled by such a choice. A simple chain of M atoms would have $M - 1$ stretching coordinates, $M - 2$ bending angles, and $M - 3$ torsions, or a total of $3M - 6$ internal degrees of freedom as desired. Branched chains would also fulfill that criterion. However, in molecules containing rings the situation is different. In a "simple" ring of M atoms one can construct M stretches, M bends, and M torsions. Obviously not all of them are independent. It is quite easy to see that there are M independent stretches and $M - 3$ of each of the torsions and bends. There is no unique choice of the six angular modes to be removed, but in a ring possessing symmetry the redundant coordinates should clearly be chosen to be symmetry adapted so that the remainder can also be described in symmetry coordinates. This can be accomplished by removing the angular and torsional combinations of A and E_1 symmetry. It has been suggested by Pulay and co-workers to use the same criterion for rings where the actual point-group symmetry is not present, leading to the concept of "natural internal coordinates".[9,15] We have used that approach to generate coordinates in our calculations and have found it a very powerful tool for converging several notoriously difficult systems.

TABLE II: Selected Equilibrium Geometry Parameters[a] of Some of the Benchmark Molecules Shown in Figure 1, Obtained by Different Basis Sets[b]

molecule	parameter	STO-3G	3-21G	minimal	6-31G**
fa	r_1	1.2167	1.2069	1.2548	1.1845
	r_2	1.1014	1.0832	1.1714	1.0934
ac	r	1.2188	1.2111	1.2499	1.1924
hp	r	1.3963	1.4731		
	τ	125.00	180.00		
2w	r	1.7503	1.8252	1.4672	
	α_1	100.39	107.87	112.43	
	α_2	110.89	110.01	120.50	
	α_3	179.70	175.90	179.94	
dp1	τ_1	177.38	188.90		
	τ_2	206.54	164.52		
	τ_3	180.49	230.77		
	τ_4	183.67	181.18		

[a] Bond lengths r are given in Å, bond angles α and torsions τ in degrees. Torsions are defined as normalized sum of all possible dihedral angles.[15] [b] Standard basis sets (see refs 20, 21, and 22 for STO-3G, 3-21G, and 6-31G**, respectively); minimal basis: 2s contracted to 1s for H; 4s/2p contracted to 2s/1p for C,O.[23]

III. Results and Discussion

Geometry optimization of formaldehyde (fa), an acetone (ac) conformer, and a condensed ring system (dye) have been carried out. For symmetry reasons in these molecules only hard modes, containing angular bond stretching and angle deformation coordinates, had to be optimized. To investigate the optimization efficiency of molecules having soft modes (torsions, out-of-planes, weak bonds), the hydrogen-bonded water dimer (2w), the hydrogen fluoride dimer (2hf), and the ethylene–water dimer (e2w) complexes as well as the hydrogen peroxide (hp) molecule have been optimized. Geometries of peptides are often difficult to optimize, due to the presence of several torsions and out-of-plane modes as well as of intramolecular hydrogen bonds. For that reason we investigated the convergence behavior of two small dipeptide (dp1, dp2) examples. In a recent paper[16] Baker and Hehre reported a comparative study of geometry optimization methods on a fused nonplanar bicyclic ring system containing sulfur and nitrogen atoms (ACTHCP), a structure problem claimed to be very difficult. The geometry optimization of that molecule has been repeated with our approach for comparison. The computation of the equilibrium geometry of $C_{16}H_{26}OSSi$, a molecule with 129 independent internal degrees of freedom including a ring system, and several soft modes, is the most complex structure optimization presented here. The molecules mentioned above are represented in Figure 1.

The influence of the initial nuclear Hessian, the choice of the coordinate system on the optimization progress, and the performance of the SO, DIIS, and combined SO/DIIS methods were investigated for some of these molecules. Comparisons with first-order methods implemented in the Gaussian 88,[17] CADPAC 4.2,[18] and SPARTAN[19] programs and with a full second-order method (explicit evaluation of the second derivatives) were made. The optimizations were carried out using a van Duijneveldt minimal basis, STO-3G, 3-21G, 3-21G*, or 6-31G** basis sets (see Table II) starting from either a fully optimized geometry obtained by yet another basis set mentioned here, a semiempirical or an experimental geometry. The convergence criterion was always 10^{-5} au for the largest element of the nuclear gradient vector in Cartesian coordinates and for the orbital gradient vector. By use of these fairly different basis sets as well as semiempirical or experimental starting structures, the changes in the geometry

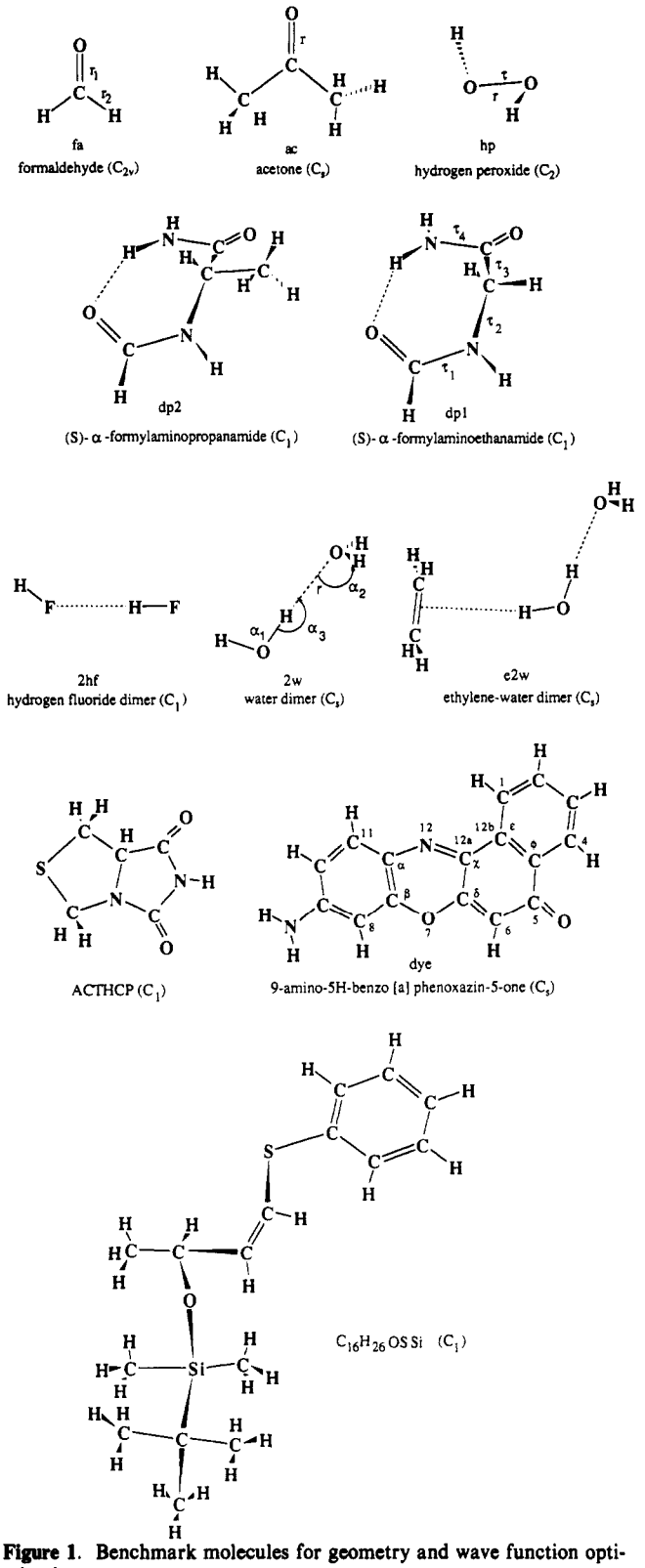

Figure 1. Benchmark molecules for geometry and wave function optimization.

parameters are not small, especially if soft modes are present (see Table II).

Unit Matrix as Initial Nuclear Hessian. An approach frequently used for the initial nuclear Hessian is the unit matrix. The information about the actual values of the force constants must be accumulated by the optimization procedure. Thus, for a given coordinate system the optimization progress depends on the difference between the exact second derivative matrix and the unit matrix. Therefore the optimization of the water dimer is considerably slower than the formaldehyde and acetone molecules due to the presence of three soft modes (see Table III). In the examples 2-3, 11-12, and 20-21 given in Table III, the DIIS method required fewer iterations than the BFGS second-order method to converge the wave function and the geometry. It is our experience from other optimizations that the DIIS adaptation outlined here is less sensitive to a poor guess for the Hessian than the SO methods. The water dimer examples 20–22 show that the performance of the DIIS method was improved by the combination with a SO method. In addition to the BFGS method, we also implemented the Murtagh–Sargent, Davidon–Fletcher–Powell, the Fletcher switch and the Hoshino SO update methods (see ref 12 for details) for both the orbital and geometry Hessian. In the majority of the cases the BFGS method was the most reliable procedure. The performance of these update procedures was either unchanged or improved by the combination with the DIIS method. We also note that starting from a unit Hessian matrix, the number of geometry steps strongly depends on the number of internal degrees of freedom (IDF) to be optimized. Comparing formaldehyde (IDF = 3) and acetone (IDF = 15), the DIIS/SO method needs about twice the number of geometry steps (see examples 4 and 13).

Empirical Initial Nuclear Hessian. As outlined in section II, empirical nuclear Hessians can be generated by redundant individual internal force constants to very low computational costs. Without hydrogen bonds nearly the same number of geometry steps was required (see examples 5–10, 14–19, and 38–39 in Table III) using either the formulas given by Schlegel[10] (for negative individual force constants the absolute values were assigned) or the formulas given in Table I. In the case of the hydrogen-bonded dimers significant improvements were obtained (examples 23–32) using the formulas presented here.

As discussed above, the number of geometry steps strongly depends on the number of internal degrees of freedom with a unit matrix as an initial guess for the Hessian. With an empirical initial Hessian, significantly fewer geometry steps were observed (see examples 5–10 and 14–19). For an extended ring system like the "dye" example (IDF = 57) only 10 geometry steps were needed. The same observation was made for molecules containing weak bonds and soft modes like the water dimer (IDF = 8) in comparison to the ethylene–water dimer complex (IDF = 18) and between the two dipeptide examples (IDF = 33 and 42, respectively) given in Table III. The geometry optimization of $C_{16}H_{26}OSSi$ required 20 geometry cycles starting from a semiempirical MNDO[25] geometry. This large and difficult example also indicates that the number of iterations is nearly independent of the number of degrees of freedom to be optimized.

The dipeptide dp1 example was used to investigate the performance of the DIIS, SO, and combined DIIS/SO method starting from a reasonable initial Hessian. Taking into account the large changes in the torsions and out-of-plane geometry parameters (see Table II) this is a realistic and a challenging geometry optimization. Although the DIIS method performed well in the first iterations, the method was not able to reach the required convergence criterion of 10^{-5} au within 30 geometry steps (see example 33). The BFGS method performed significantly better for this example (no. 34). The torsion and out-of-plane angles changed less than 0.01° when convergence was reached. Whether one starts from a poor or a reasonable Hessian guess, the DIIS/SO algorithm outperforms the individual SO and DIIS methods, because of the capability to combine the robustness of the DIIS method with the accumulation of second derivative information (see also no. 35). We also compared the SO/DIIS algorithm with the usual density matrix based DIIS method[6] for wave function optimization at a given geometry. Starting from an orbital gradient vector norm less than 1.0 au, both these methods showed very similar performance. For poor guesses of a start wave function, the density matrix based DIIS or any other damped SCF procedure[28] is more robust and should be initially used until the orbital gradient norm is less than about 1.0 au.

Choice of the Coordinate System for Geometry Optimizations. Another important topic is the choice of coordinate basis for a geometry optimization. As mentioned above we applied pseudosymmetry adapted linear combinations of internal coordinates,

TABLE III: Performance of the Geometry Optimization[a] of the Benchmark Molecules Using Different Basis Sets, Initial Inverse Nuclear Hessians, Coordinate Systems, and Optimization Methods[a]

no.	initial geometry[b,c]	basis set[c]	Hessian[d]	coordinate system[e]	method[f]	no. of GRD[g]	no. of SCF[h]
			Formaldehyde (IDF[i] = 3)				
1	STO-3G	3-21G	unit	internal	steepest descent[j]	35	82
2	STO-3G	3-21G	unit	internal	BFGS	10	40
3	STO-3G	3-21G	unit	internal	DIIS	7	31
4	STO-3G	3-21G	unit	internal	BFGS/DIIS	7	31
5	STO-3G	3-21G	estim*	internal	BFGS/DIIS	4	19
6	STO-3G	3-21G	estim**	internal	BFGS/DIIS	6	24
7	3-21G	minimal	estim*	internal	BFGS/DIIS	6	27
8	3-21G	minimal	estim**	internal	BFGS/DIIS	5	24
9	minimal	6-31G**	estim*	internal	BFGS/DIIS	6	29
10	minimal	6-31G**	estim**	internal	BFGS/DIIS	6	29
			Acetone (IDF = 15)				
11	STO-3G	3-21G	unit	internal	BFGS	16	53
12	STO-3G	3-21G	unit	internal	DIIS	13	48
13	STO-3G	3-21G	unit	internal	BFGS/DIIS	13	48
14	STO-3G	3-21G	estim*	internal	BFGS/DIIS	6	31
15	STO-3G	3-21G	estim**	internal	BFGS/DIIS	6	28
16	3-21G	minimal	estim*	internal	BFGS/DIIS	7	35
17	3-21G	minimal	estim**	internal	BFGS/DIIS	7	33
18	minimal	6-31G**	estim*	internal	BFGS/DIIS	7	37
19	minimal	6-31G**	estim**	internal	BFGS/DIIS	7	36
			Water Dimer (IDF = 8)				
20	STO-3G	3-21G	unit	internal	BFGS	28	108
21	STO-3G	3-21G	unit	internal	DIIS	25	102
22	STO-3G	3-21G	unit	internal	BFGS/DIIS	21	90
23	STO-3G	3-21G	estim*	internal	BFGS/DIIS	8	41
24	STO-3G	3-21G	estim*	cart.	BFGS/DIIS	11	55
25	STO-3G	3-21G	estim**	internal	BFGS/DIIS	12	58
26	3-21G	minimal	estim*	internal	BFGS/DIIS	11	51
27	3-21G	minimal	estim**	internal	BFGS/DIIS	14	70
			Ethylene–Water Dimer (IDF = 18)				
28	STO-3G	3-21G	estim*	internal	BFGS/DIIS	11	60
29	STO-3G	3-21G	estim**	internal	BFGS/DIIS	16	80
30	3-21G	minimal	estim*	internal	BFGS/DIIS	14	80
			HF Dimer (IDF = 6)				
31	ref 24	DZP[m]	estim*	internal	BFGS/DIIS	8	46
32	ref 24	DZP[m]	estim**	internal	BFGS/DIIS	11	60
			(*S*)-α-Formylaminoethanamide (IDF = 33)				
30	STO-3G	3-21G	estim*	internal	DIIS	>30	>150
31	STO-3G	3-21G	estim*	internal	BFGS	21	116
32	STO-3G	3-21G	estim*	internal	BFGS/DIIS	18	105
33	STO-3G	3-21G	estim*	cart.	BFGS/DIIS	29	149
			(*S*)-α-Formylaminopropanamide (IDF = 42)				
34	STO-3G	3-21G	estim*	internal	BFGS/DIIS	19	107
			Hydrogen Peroxide (IDF = 4)				
35	STO-3G	3-21G	estim*	internal	BFGS/DIIS	11	57
36	STO-3G	3-21G	estim**	internal	BFGS/DIIS	11	57
			9-Amino-5*H*-benzo[*a*]phenoxazin-5-one (IDF = 57)				
37	STO-3G	3-21G	estim*	internal	BFGS/DIIS	10	57
			ACTHCP (IDF = 42)				
38	exp[k]	STO-3G	estim*	internal	BFGS/DIIS	25	132
			$C_{16}H_{26}OSSi$ (IDF = 129)				
39	MNDO[25]	3-21G*[l]	estim*	internal	BFGS/DIIS	20	140

[a] The starting geometries used were obtained through full geometry optimization using the basis sets given in column 1. [b] Convergence was assumed if the largest component of both the orbital and nuclear Cartesian gradient vector was less than 10^{-5} au. [c] See Table II. [d] Initial nuclear inverse Hessian. Either the unit matrix (unit) or an empirically estimated Hessian obtained by different formulas (estim*, see Table I; estim**, formulas given by Schlegel[10]). [e] Nuclear coordinate system used for the optimization. Either symmetry-adapted internal coordinates (internal) or Cartesian coordinates. [f] Optimization algorithm for both orbital and geometry parameters. See text for details. [g] Total number of nuclear gradient evaluations required to reach convergence. [h] Total number of SCF iterations within the geometry optimization starting from an initial wave function guess converged to 1.0 au of the norm of the orbital gradient vector. [i] Internal degrees of freedom to be optimized within the underlying symmetry (see Figure 1). [j] Only used for geometry parameters. The orbital parameters were optimized using the BFGS algorithm. [k] Taken from the Cambridge Structural Data Base.[26] [l] Polarization functions used for sulfur and silicon. [m] The basis set used for fluorine was the 9s5p1d DZP basis of Dunning[27] augmented with a diffuse s, p, and d function (exponents, 0.12, 0.09, 0.40) and the correspondent 4s1p basis for hydrogen augmented by a diffuse s and p function (exponents 0.06 and 0.275).

"natural internal coordinates", in our optimization. A comparison of the efficiency of a geometry optimization using Cartesian coordinates was made for the water dimer and the dp1 example (see Table III, examples 24 and 36). In order to get a comparable initial inverse nuclear Hessian, the Cartesian force constant matrix in eq 7 can be inverted by any pseudoinversion method. Small

TABLE IV: Number of Wave Function Optimization Cycles (SCF) per Geometry Step Required for the Geometry Optimization of the Acetone and the Water Dimer[a]

	acetone		water dimer	
step[b]	Gaussian88[c] SCF	BFGS/DIIS[d] SCF	CADPAC4.2[e] SCF	BFGS/DIIS[d] SCF
initial	11	14	11	13
1	10	6	9	7
2	10	5	8	6
3	12	5	8	5
4	12	4	7	4
5	5	3	7	4
6		8	4	
7		7	3	
8		6		
9		5		

(*S*)-α-Formylaminopropanamide

	full second-order[f]	BFGS/DIIS
no. of GEO[g]	8	19
no. of SCF[h]	191	97

[a] Both examples use a 3-21G basisset, and start from the optimized STO-3G geometry. A comparison of the BFGS/DIIS procedure to other first-order optimization procedures and to a full second-order method by means of the (*S*)-α-formylaminopropanamide example. [b] The number of the geometry step starting from initial geometry. [c] Gaussian88 direct method using the Pulay extrapolation scheme and the Schlegel geometry optimization procedure. Convergence for the wave function was assumed if the root mean square difference in the density matrices between two consecutive steps was less than 10^{-7} au. Convergence in the geometry parameters was assumed if the largest component of the Cartesian nuclear gradient vector was less than 10^{-5} hartree/bohr. [d] Convergence was assumed if the largest component of both the orbital and Cartesian nuclear gradient vector was less than 10^{-5} au. The initial wave function guess was taken from atomic density. [e] Standard geometry optimization procedure starting from an analytic calculated second derivative matrix. Convergence for the wave function was assumed if the largest change in density matrix was less than 10^{-6} au. Convergence in the geometry parameters was assumed if the largest component of the Cartesian nuclear gradient vector was less than 10^{-5} hartree/bohr. [f] Quadratic convergent second-order method.[30] [g] Total number of geometry steps or macroiterations for the full second-order method (see ref 30 for details). [h] Total number of SCF iterations or microiterations for the full second-order method (see ref 30 for details) beginning with a 3-21G converged wave function.

molecules like formaldehyde showed no differences in the required geometry steps, whereas the water dimer and especially the dp1 molecule performed significantly worse if optimized in Cartesian coordinates.

For the multiple ring system "dye" we used nonlocal ring coordinates as discussed above. Although the dye system has only C_s symmetry, we used the 18 ring of the 5*H*-benzo[*a*]phenoxazin framework (see Figure 1) as a basis for our ring coordinate definition. The ring substituent coordinates were defined as suggested by Pulay.[9,15] The bond stretch coordinates between the atoms α and β, χ and δ, ε and φ as well as angle deformations and torsions of these bonds were not involved in the $3N - 6$ linear independent coordinates. In order to take the forces caused by these regular chemical bonds into account, they were included in the individual internal coordinates (see eq 7). In a very similar way we proceeded in the ACTHCP example. Using the SPARTAN program,[19] the authors report that in the best case, working with Cartesian coordinates, 90 geometry cycles were required to converge this molecular structure.[24] With the algorithm described here, only 16 iterations were needed to converge the structure to 2×10^{-4} au (which is approximately the criterion used in ref 16) and 25 cycles were required to reach a convergence criterion of 10^{-5} au. This excellent result is mainly due to the use of natural internal coordinates. Optimizations of other multiple ring systems, e.g., different tautomers of chlorin,[29] could also be done within less than 10 iterations using the same procedure.

Comparison to Other Optimization Methods. We have compared the number of wave function optimization cycles (#SCF) required in each step of a complete geometry optimization with methods implemented in the Gaussian 88 and CADPAC 4.2 program packages (see Table IV). For that purpose we chose the acetone and water dimer example, because all optimizations required approximately the same number of geometry iterations. Table IV shows that except for the initial geometry, where DISCO apparently starts from a worse guess for the wave function, the SO/DIIS method needs considerably fewer SCF iterations. This is mainly because DISCO carries the orbital Hessian over into subsequent geometry cycles, which allows for increasingly faster SCF convergence. Furthermore, a comparison with a simultaneous full second-order method applied to the dp2 case[30] shows that for this difficult example about 2–3 times the number of geometry steps were indeed required but only half of the orbital steps. This assumes that the time required for an orbital step is about the same as for a microiteration for the full second-order method.

Based on the similarity of the wave function and geometry optimization procedures it is also possible to optimize these parameters simultaneously.[5] Then the total Hessian contains coupling terms of nuclear and orbital Hessian and can be updated by the total energy gradient vector. We found that the SO/DIIS method works also very well for the simultaneous optimization. In general, this method leads to an increase of the required geometry steps and to a reduction of required SCF iterations in comparison to the conventional algorithm. Therefore the efficiency strongly depends upon the time ratio between SCF and nuclear gradient evaluation.

IV. Conclusions

This study provides a competitive algorithm for a wave function optimization within a geometry optimization by reusing second derivative information gained from the wave function optimization on previous geometries. The recursive formulation of this algorithm requires only a small amount of memory and is therefore very well suited for the application on large molecular systems within the framework of direct SCF calculations.

This investigation shows that the combination of DIIS extrapolation scheme and the second-order update method for both wave function and geometry optimization outperforms the individual DIIS and second-order update procedures. In addition, we introduce a new parameterization for the initial nuclear Hessian and investigate methods for the generation of symmetry-adapted internal coordinates for large ring systems. By means of a series of benchmark molecules, we quantitatively show that the efficiency of a geometry optimization algorithm equivalently depends on the initial inverse Hessian, on the coordinate system choice, and on the optimization procedure. A significant reduction in the required geometry steps can be obtained by using an empirical initial nuclear Hessian matrix as well as symmetry-adapted internal coordinates and the SO/DIIS update method. No dependency of the number of geometry cycles on the number of degrees of freedom to be optimized is observed.

Acknowledgment. The calculations were carried out on Cray-2 computers at the Minnesota Supercomputer Center and at the National Center for Supercomputing Applications, Urbana-Champaign. This work was supported by the National Science Foundation, Grant No. CHE-8915629, and by the Deutsche Forschungsgemeinschaft.

References and Notes

(1) Almlöf, J.; Faegri, K., Jr.; Korsell, K. *J. Comput. Chem.* **1982**, *3*, 385.
(2) Head-Gordon, M.; Pople, J. A.; Frisch, M. J. *Chem. Phys. Lett.* **1988**, *153*, 503. Saebø, S.; Almlöf, J. *Chem. Phys. Lett.* **1989**, *154*, 83.
(3) Thouless, D. J. *Nucl. Phys.* **1960**, *21*, 225.
(4) Douady, J.; Ellinger, Y.; Subra, R.; Levy, B. *J. Chem. Phys.* **1980**, *72*, 1452. Bacskay, G. B. *Chem. Phys.* **1981**, *61*, 385.
(5) Head-Gordon, M.; Pople, J. A. *J. Phys. Chem.* **1988**, *92*, 3063.
(6) Pulay, P. *Chem. Phys. Lett.* **1980**, *73*, 393. Pulay, P. *J. Comput. Chem.* **1982**, *3*, 556.
(7) Csaszar, P.; Pulay, P. *J. Mol. Struct.* **1984**, *114*, 31.
(8) Cummins, P. L.; Gready, J. E. *J. Comp. Chem.* **1989**, *10*, 939.
(9) Fogarasi, G.; Zhou, X.; Taylor, P. W.; Pulay, P. *J. Am. Chem. Soc.* in press.
(10) Schlegel, H. B. *Theor. Chim. Acta* **1984**, *66*, 333.

(11) Almlöf, J.; Faegri, K., Jr.; Feyereisen, M. W.; Fischer, T. H.; Korsell, K.; Lüthi, H. P. DISCO, a direct SCF and MP2 code.
(12) Fletcher, R. *Practical Methods of Optimization*; Wiley: New York, 1980; Vol. 1.
(13) Pulay, P. *Mol. Phys.* **1969**, *17*, 197.
(14) Califano, S. *Vibrational States*; Wiley: New York, 1976; Chapter 4.
(15) Pulay, P.; Fogarasi, G.; Pang, F.; Boggs, J. E. *J. Am. Chem. Soc.* **1979**, *101*, 2550.
(16) Baker, J.; Hehre, W. J. *J. Comput. Chem.* **1991**, *12*, 606.
(17) Frisch, M. J.; Head-Gordon, M.; Schlegel, H. B.; Raghavachari, K.; Binkley, J. S.; Gonzalez, C.; DeFrees, D. J.; Fox, D. J.; Whiteside, R. A.; Seeger, R.; Melius, C. F.; Baker, J.; Kahn, L. R.; Stewart, J. J. P.; Fluder, E. M.; Topiol, S.; Pople, J. A. *Gaussian 88*; Gaussian Inc.: Pittsburgh, PA, 1988.
(18) Amos, R. D.; Rice, J. E. *CADPAC: The Cambridge Analytic Derivatives Package*; issue 4.2, Cambridge, 1990.
(19) Carpenter, J. E.; Baker, J.; Hehre, W. J.; Kahn, S. D. *The SPARTAN System*, 1990.
(20) Hehre, W. J.; Stewart, R. F.; Pople, J. A. *J. Chem. Phys.* **1969**, *51*, 2657.
(21) Binkley, J. S.; Pople, J. A.; Hehre, W. J. *J. Am. Chem. Soc.* **1980**, *102*, 939.
(22) Francl, M. M.; Pietro, W. J.; Hehre, W. J.; Binkley, J. S.; Gordon, M. S.; DeFrees, D. J.; Pople, J. A. *J. Chem. Phys.* **1982**, *77*, 3654.
(23) van Duijneveldt, F. B. IBM Publication RJ 945 (No. 16437).
(24) Diercksen, G. H. F.; Krämer, W. *Chem. Phys. Lett.* **1970**, *6*, 419.
(25) Dewar, M. J. S.; Thiel, W. *J. Am. Chem. Soc.* **1977**, *99*, 4899.
(26) Allen, F. H.; Bellard, S.; Brice, M. D.; Cartwright, B. A.; Doubleday, A.; Higgs, H.; Hummelink, T.; Hummelink-Perrers, B. A.; Kennard, O.; Motherwell, W. D. S.; Rodgers, J. R.; Watson, D. A. *Acta Crystallogr., Sect. B* **1979**, *35*, 2331.
(27) Dunning, T. H. *J. Chem. Phys.* **1970**, *53*, 2823.
(28) Sellers, H. *Chem. Phys. Lett.* **1991**, *180*, 461.
(29) Fischer, T. H.; Ghosh, A.; Almlöf, J.; Gassman, P. G. *J. Am. Chem. Soc.* (in press).
(30) Head-Gordon, M.; Pople, J. A.; Frisch, M. J. *Int. J. Quantum Chem., Symp.* **1989**, *23*, 291.

Structure, Spectra, and Stability of Ar_2H^+, Kr_2H^+, and Xe_2H^+: An Effective Core Potential Approach

Jan Lundell*,† and Henrik Kunttu‡,§

Departments of Physical Chemistry and Medical Chemistry, University of Helsinki, SF-00170 Helsinki, Finland *(Received: May 22, 1992)*

The molecular properties of Ar_2H^+, Kr_2H^+, and Xe_2H^+ are studied in their electronic ground states by ab initio methods using the effective core potential approach or all-electron methods employing the STO-3G* and 6-31G** Gaussian basis sets. Linear structures are obtained for these ions at all levels of computational theory. The lowest energy geometry is that where hydrogen is located between the rare gas atoms: for Kr_2H^+ and Xe_2H^+, this structure is centrosymmetric ($D_{\infty h}$), whereas for Ar_2H^+ some of the calculations show unequal Ar–H distances. The collinear Rg···(Rg–H)$^+$ local minimum, possessing a minimal amount of charge delocalization among the rare gas atoms, was found to be 0.2–0.4 eV higher in energy. Predictions concerning the vibrational frequencies of the different structures are made. For all three species, the calculated σ_g and σ_u frequencies support the experimental assignments. Based of the potential energy surface computed for Ar_2H^+, an isomerization mechanism involving the correlated motion of the nuclei is suggested as the origin of the observed thermal instability of these ions.

I. Introduction

Ionic rare gas clusters have become the subject of a vigorously expanding field of research during the recent years. The advent of experimental procedures such as supersonic expansions and time-of-flight techniques has greatly enhanced the feasibility of experiments of high size selectivity.[1-6] From the theoretical viewpoint, a significant computational effort toward a rigorous understanding of these systems at the microscopical level has been pursued.[7] Particularly, ionic clusters trapped in condensed phases provide a rather fascinating interface between isolation and continuous matter and, as such, enable a detailed insight to a wide variety of many-body interactions involved in chemical reaction dynamics in general. Moreover, the mundane issue of energy storage is closely tied to these highly energetic species.[8]

In the preceding paper, herein referred to as 1,[9] we demonstrated that delocalized charge-transfer excitations in solid xenon, multiply doped with atomic halogens (I, Br, Cl) and hydrogen, lead to permanent charge separation by trapping of the positive charge. The trapped state was ascribed to a triatomic Xe_2H^+ molecular ion, a member of a larger family of ionic clusters of the form Xe_nH^+ recently described in the framework of diatomics in ionic systems (DIIS) by Last and George.[10] In analogy with the isoelectronic species IHI^-,[11,12] the observed prominent progression of absorptions in the 700–1200-cm^{-1} region was assigned to a $\nu_3 + n\nu_1$ (n = 0–4) progression of combination bands of a linear $(Xe–H–Xe)^+$ ion of $D_{\infty h}$ symmetry. Once this species was generated, its spectral features were found to be virtually insensitive to the type of halogen in the initial parent, HX (X = I, Br, Cl), molecule. The proposed geometry is, indeed, in deep contrast with the recent DIIS computation predicting a linear structure composed of a deeply bound XeH^+ unit loosely bound to a essentially neutral Xe atom on the rare gas side.[10] One of the most interesting findings presented in 1 is the observed decomposition of Xe_2H^+ in the dark at temperatures near 10 K. Quite interestingly, this process was observed for the protonated ion only. Although not completely understood, the dark decay of Xe_2H^+ absorptions was, a priori, ascribed to a tunneling mechanism involving the internal coordinate of the ion. The early matrix isolation data on Ar_2H^+ and Kr_2H^+ showed the same kind of thermal instability.[13]

Most of the theoretical approaches concerning ionic rare gas–hydrogen clusters limit themselves to a description of argon species.[8,14,15] The most recent ab initio treatment by Rosenkrantz[8] gives the optimized geometries of ArH^+, Ar_2H^+, and Ar_4H^+ using several basis sets at different levels of computational theory. Also, predictions of the harmonic vibrational frequencies are given. Even for the triatomic ion, the optimized structure is not, however, stable at all levels of approximation. For the heavier rare gases, the current literature is more sparse, and ab initio investigations exist for the experimentally known diatomic KrH^+ and XeH^+ ions only. Nevertheless, the detailed studies by Rosmus and co-workers[16-18] utilizing highly correlated SCEP/VAR (self-consistent electron pair approach yielding variational results) and SCEP/CEPA (coupled electron approach) methods are in excellent agreement

† Department of Physical Chemistry.
‡ Department of Medical Chemistry.
§ Permanent address: Department of Physical Chemistry, University of Helsinki, SF-00170 Helsinki, Finland.

0022-3654/92/2096-9774$03.00/0